THE JOURNAL OF PHYSICAL CHEMISTRY A

Article

pubs.acs.org/JPCA

Calixarene-Based Fluorescent Sensors for Cesium Cations Containing BODIPY Fluorophore

Alexis Depauw,[†] Naresh Kumar,[†] Minh-Huong Ha-Thi,*[,†,‡] and Isabelle Leray*[,†]

[†]PPSM (CNRS UMR 8531), ENS Cachan, 61 Avenue du Président Wilson, 94230 Cachan, France

[‡]Institut des Sciences Moléculaires d'Orsay - ISMO (CNRS UMR 8214), Université de Paris Sud, Bâtiment 210, 91405 Orsay Cedex, France

Supporting Information

ABSTRACT: New fluorescent molecular sensors based on a calix[4]arene biscrown-6 ether as coordination site and BODIPY derivative as signaling unit were synthesized, and their photophysical properties were characterized. The complexation properties of these sensors with potassium and cesium cations were investigated using both steady-state and time-resolved fluorescence methods. The studies show that the sensitivity with cations depends upon the position of substituted coordination site on the BODIPY core. The complexation with cations does not have much effect on the absorption and emission wavelength when the coordination site (calix[4]arene biscrown-6 ether) is introduced at the *meso* position of the BODIPY core. In contrast, the same calix[4]arene biscrown-6 ether attached via a styryl linker to the α-position of BODIPY core leads to a sensitive sensor for alkali cations thanks to the better conjugation between the coordination site and the BODIPY core. The complexation of cations induces a hypsochromic shift of the absorption and emission maximums due to the diminution of donor character of the oxygen atoms in the coordination site. The stability constants of complexes with potassium and cesium ion were measured.

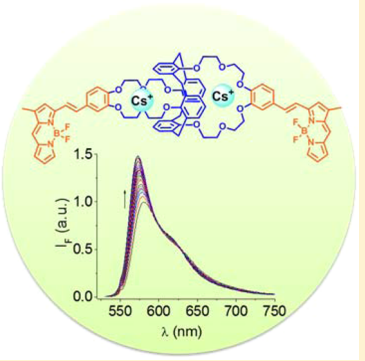

INTRODUCTION

The detection of cesium is of great interest because of its intrinsic toxicity. The major source of cesium involves nuclear waste materials. The accident of the Fukushima Nuclear Power plant following the Tohoku tsunami in March 2011 lead to a major release of radioactive material, including Cs^+. The cesium toxicity is due to its ability to replace potassium in muscles and red blood cells, which is responsible for the cardiac and cancerogenic diseases.[1,2] The cesium level can be determined by different methods such as atomic absorption spectroscopy[3] and radioanalysis.[4,5] In this context, the use of fluorescent sensor[6−9] has several advantages in terms of sensitivity, selectivity, and response time.

A typical fluorescence sensor consists of a recognition site (ionophore) combined to a signaling unit (fluorophore).[6,7] Among the recognition sites, the calix[4]arene biscrown-6 ether was shown to have a good selectivity for alkali cations, especially for cesium.[10−12] We previously reported different calix[4]arene biscrown-6 ether in which a coumarin fluorophore is introduced into both crown-ethers.[13,14] These molecules exhibit high selectivity for cesium cations with the limitation that their excitation wavelength falls in the UV region. Meanwhile, the design of visible and near-infrared fluorescence molecular sensors for alkali cations has received increasing attention because of their potential applications in biology and the environment. Indeed, the utility of fluorescent probes excited in UV wavelength region is limited by the footprint size, portability, power consumption, and by the expense of ultraviolet lasers for practical and field applications. In particular, probes having longer excitation wavelength are desirable as they have enabled the use of laser diodes (LD) instead of light-emitting diodes (LED) in microdevices for the development of portable sensors for environment applications.[15,16] These LDs, widely available at visible wavelength, offer distinct advantages, including a higher power and a better launching in optical fiber comparing to LEDs.

BODIPY (4,4-difluoro-4-bora-3a,4a-diaza-s-indacene) derivatives have been widely used for different applications concerning sensors,[17] biological imaging, and labeling,[18] electroluminescent devices,[19] or tunable laser dyes.[20] This family of molecules offers different advantages, including intense absorption and emission in the visible region along with high photochemical stability. In addition, their photophysical properties can be tuned by introducing functional groups at different positions of the BODIPY core.[21,22] In order to obtain fluorescent probes for cesium excitable at longer wavelength, we herein synthesize two new fluoroionophores consisting of a calix[4]biscrown-6 ether as the coordination site and a BODIPY fluorophore as the signaling unit. In these systems, the calixcrown was introduced in *meso* or α position to

Special Issue: Jean-Michel Mestdagh Festschrift

Received: December 2, 2014
Revised: January 30, 2015

DOI: 10.1021/jp5120288
J. Phys. Chem. A XXXX, XXX, XXX−XXX

the BODIPY core. The spectroscopic and complexing properties of these two ligands were investigated by different photophysical methods (absorption, fluorescence, and time-resolved fluorescence) in order to understand their photo-induced behavior. The different behavior between these two ligands in terms of photophysical changes in the presence of cations will be discussed.

EXPERIMENTAL SECTION

Synthesis. All reagents were purchased from Aldrich and were used without further purification. ^{1}H and ^{13}C spectra were recorded on a JEOL-FT NMR 400 MHz (100 MHz for ^{13}C NMR) spectrophotometer using $CDCl_3$ as a solvent and tetramethylsilane as an internal standard. Data are reported as follows: chemical shift in ppm (δ), multiplicity (s = singlet, d = doublet, t = triplet, m = multiplet, br = broad singlet), and coupling constants J (Hz).

25,27:26,28-Bis(benzaldehyde-3,4-bis(2-(2-oxyethoxy)-ethoxy))calix[4]arene ***2***. In a round-bottom flask under argon, 3.1 g (7.3 mmol) of calix[4]arene and 16.0 g (116.1 mmol) of potassium carbonate in dry acetonitrile (400 mL) were stirred for 1 h at room temperature. 9.0 g (14.5 mmol) of Ditosylate **1** in dry acetonitrile (100 mL) were then added and the reaction mixture was refluxed for 6 days. The solvent was then removed under reduced pressure, the mixture treated with a 1 M HCl solution, water, and extracted with CH_2Cl_2. The organic layer was dried over anhydrous $MgSO_4$ and evaporated to dryness. The crude product was purified by chromatography on a silica gel (CH_2Cl_2−CH_2Cl_2/EtOAc 6:4) to afford 4.0 g (76%) of a white solid. NMR ^{1}H (400 MHz, $CDCl_3$): δ (ppm) 9.88 (s, 2H, CHO), 7.51 (dd, $^{4}J_{HH}$ = 1.8 Hz, $^{3}J_{HH}$ = 8.2 Hz, 2H, CH_{ar}), 7.49 (d, $^{4}J_{HH}$ = 1.8 Hz, 2H, CH_{ar}), 7.07−7.04 (m, 10H, $CH_{ar\text{-}calix}$ + CH_{ar}), 6.64 (t, $^{3}J_{HH}$ = 7.8 Hz, 4H), 4.23−4.17 (m, 8H, OCH_2), 3.81−3.75 (m, 16H, $CH_{2\text{-}calix}$ + OCH_2), 3.62−3.56 (m, 16H, OCH_2). NMR ^{13}C (100 MHz, $CDCl_3$): δ (ppm) 190.97, 156.58, 154.47, 149.42, 134.18, 134.12, 130.63, 130.25, 127.07, 122.41, 112.83, 112.21, 70.60, 70.39, 70.27, 69.97, 69.92, 69.69, 69.58, 37.77. HRMS (TOF MS ES+): calculated for $C_{58}H_{60}O_{14}$, 980.4042; found, 980.3983.

Calix-BODIPY-S. In a round-bottom flask under argon, 200 mg (0.2 mmol) of **2** and 175 mg (0.8 mmol) of 1,3-dimethylbodipy were stirred in 5 mL toluene. Ten microliters (0.06 mmol) of piperidine were then added, and the mixture was refluxed for 20 h, until complete consumption of the starting aldehyde was observed by thin layer chromatography (TLC). The toluene was removed under reduced pressure, and the crude product was directly purified by chromatography on a silica gel with the following eluent (CH_2Cl_2−CH_2Cl_2/EtOAc 6:4) to afford after precipitation 35 mg (12%) of purple crystals. See the structure in Figure 1. NMR ^{1}H (400 MHz, $CDCl_3$): δ (ppm) 7.66 (s, 2H, CH_{ar}), 7.55−7.50 (d, $^{3}J_{HH}$ = 16.2 Hz, 2H), 7.38−7.33 (d, $^{3}J_{HH}$ = 17.4 Hz, 2H), 7.15 (s, 2H, CH_{ar}), 7.10−7.06 (m, 12H, $4CH_{ar}$ + $8CH_{ar\text{-}calix}$),), 6.98−6.96 (d, $^{3}J_{HH}$ = 8.4 Hz, 2H, CH_{ar}), 6.91, (d, $^{4}J_{HH}$ = 3.2 Hz, 2H, CH_{ar}), 6.76 (s, 2H, CH_{ar}), 6.71−6.67 (t, $^{3}J_{HH}$ = 7.56 Hz 4H, $CH_{ar\text{-}calix}$), 6.45 (s, 2H, CH_{ar}), 4.18 (m, 8H, OCH_2), 3.77 (m, 16H, OCH_2 + CH_2), 3.71−3.69 (m, 4H, OCH_2), 3.63−3.61 (m, 4H, OCH_2), 3.58−3.53 (m, 8H, OCH_2), 2.33 (s, 6H, CH_3). NMR ^{13}C (100 MHz, $CDCl_3$): δ (ppm) 159.30, 156.47, 151.34, 149.21, 144.61, 140.19, 138.46, 138.06, 134.20, 133.07, 130.30, 129.80, 125.53, 123.50, 122.61, 122.54, 117.31, 116.95, 116.29, 114.33, 113.99, 70.42, 70.30, 70.29, 70.18, 70.09, 69.75, 37.88, 11.60. HRMS (TOF MS ES+): calculated for $C_{80}H_{78}B_2F_4N_4O_{12}$, 1384.5783; found, 1384.5786.

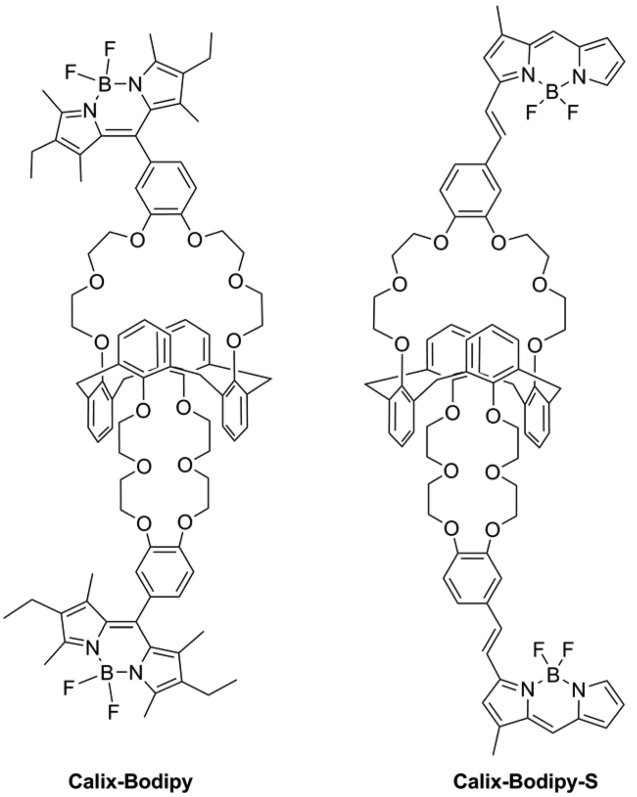

Figure 1. Structure of Calix-BODIPY and Calix-BODIPY-S.

Calix-BODIPY. In a round-bottom flask under argon were introduced 0.5 g (0.5 mmol) of **2**, 275 μL (2 mmol) of 3-ethyl-2,4-dimethylpyrole (kryptopyrole), and 15 mL of CH_2Cl_2. Once all reactants were dissolved, a catalytic amount of trifluoroacetic acid (TFA) (a few drops) was added, and the reaction was stirred at room temperature until complete consumption of the aldehyde (TLC analysis). After 40 min, 125 mg (0.5 mmol) of chloranil was added and 5 min later, 620 μL (3.6 mmol) of *N*,*N*-diisopropylethylamine (DIPEA) was added. After 30 more min, 690 μL (5.6 mmol) of $BF_3{\cdot}OEt_2$ were added, and the reaction was then stirred for 2 h at room temperature. The reaction was quenched by addition of water. The product was extracted with CH_2Cl_2 washed with water, dried over $MgSO_4$, and concentrated under reduced pressure. The crude product was first purified by column chromatography on silica gel (CH_2Cl_2−CH_2Cl_2/EtOAc 2:8) and then precipitated with diethyl ether, to afford 280 mg (35%) of a purple solid. See the structure in Figure 1. NMR ^{1}H (400 MHz, $CDCl_3$): δ (ppm) 7.21 (m, 2H, CH_{ar}), 7.05−6.99 (m, 10H, $2CH_{ar}$ + $8CH_{calix}$), 6.83 (m, 4H, $2CH_{ar}$), 6.67−6.62 (m, 4H, CH_{calix}), 4.05−4.03 (4H, m, OCH_2), 4.16−4.13 (4H, m, OCH_2), 3.76−3.70 (16H, m, OCH_2 + $CH_{2\ calix}$), 3.57−3.49 (16H, m, OCH_2), 2.47 (s, 12H, $4CH_3$), 2.22−2.27 (q, $^{3}J_{HH}$ = 7.76 Hz, 8H, $4CH_2$), 1.35 (s, 12H, $4CH_3$), 0.94−0.90 (t, $^{3}J_{HH}$ = 8 Hz, 12H, $4CH_3$). NMR ^{13}C (100 MHz, $CDCl_3$): δ (ppm) 156.51, 153.83, 149.96, 149.34, 144.95, 138.34, 134.17, 138.06, 132.80, 131.13, 130.28, 128.93, 122.45, 121.66, 114.70, 114.60, 70.39, 70.29, 70.17, 70.05, 69.91, 69.71, 37.89, 17.13, 14.72, 12.62, 11.70. HRMS (TOF MS ES+): calculated for $C_{90}H_{102}B_2F_4N_4O_{12}$, 1528.7616; found, 1528.7638.

DOI: 10.1021/jp5120288
J. Phys. Chem. A XXXX, XXX, XXX−XXX

Scheme 1. Synthetic Scheme of Calix-BODIPY and Calix-BODIPY-S

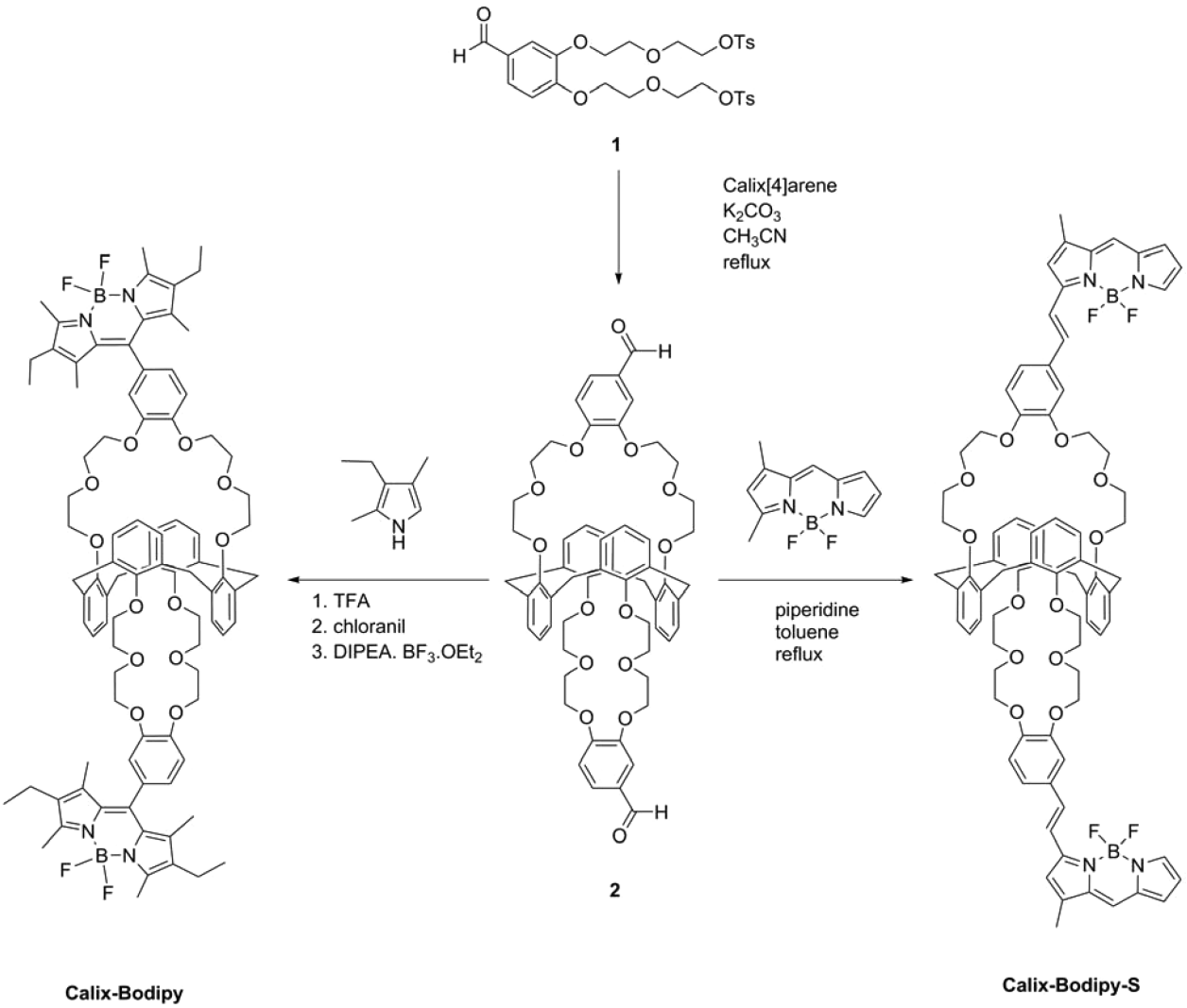

Quantum Chemical Calculations. Calculations were carried with Gaussian09[23] on a Nec TX7 with 32 processors Itanium 2 of the MESO center of the ENS Cachan. The ground state geometries were determined with DFT using B3LYP functional with a 6-31g(d) basis set. The PBE0 functional was used with a 6-311g+(d,p) basis set during TD-DFT calculations as suggested by Jacquemine et al.[24]

Solvents and Salts. Acetonitrile and dichloromethane from Aldrich (spectroscopic grade) were employed as solvent for absorption and fluorescence measurements. Cesium and potassium perchlorate from Aldrich or Alfa Aesar were of the highest quality available and vacuum-dried over P_2O_5 prior to use.

Spectroscopic Measurements. UV/vis absorption spectra were recorded on a Varian Cary5000 spectrophotometer and corrected emission spectra were obtained on a Jobin−Yvon SPEX Fluoromax-4 spectrofluorometer. The fluorescence quantum yields were determined by using Rhodamine 590 in ethanol $\Phi_F = 0.95$[25] as a reference. The complexation constants were determined by global analysis of the evolution of all absorption and/or emission spectra by using the Specfit Global Analysis System V3.0 for 32-bit Windows system. This software uses singular value decomposition and nonlinear regression modeling by the Levenberg−Marquardt method.[26] Fluorescence intensity decays were obtained by the time-correlated single-photon counting (TCSPC) method with femtosecond laser excitation using a Spectra-Physics setup composed of a Titanium Sapphire laser (Tsunami, Spectra-Physics) pumped by a doubled Nd:YVO_4 laser (Millennia *Xs*, Spectra-Physics). Light pulses at 1000 nm were selected by optoaccoustic crystals at a repetition rate of 4 MHz, and a doubling crystal is used to reach the excitation wavelength of 500 nm. Fluorescence photons were detected (at 90°) through a monochromator by means of a Hamamatsu MCP R3809U photomultiplier, connected to a SPC-630 TCSPC module from Becker & Hickl. The fluorescence data were analyzed by a nonlinear least-squares method with the aid of Globals software package developed at the Laboratory of Fluorescence Dynamics at the University of Illinois, Urbana−Champaign.

RESULTS AND DISCUSSION

Synthesis. The synthesis of the calix-BODIPY and Calix-BODIPY-S were accomplished according to the procedure displayed in Scheme 1, starting from the ditosylate **1**.[27] The calixarene **2** was obtained by carrying out the reaction of calix[4]arene with 2 equiv of ditosylate **1** in the presence of K_2CO_3 in the refluxing MeCN during 6 days. The crude product was isolated by column chromatography to afford **2** in

DOI: 10.1021/jp5120288
J. Phys. Chem. A XXXX, XXX, XXX−XXX

76% yield.[28] The synthesis of Calix-BODIPY was performed according to the procedure described by Kollmannsberger et al.[29,30] in 35% yield from 3-ethyl-2,4-dimethylpyrrole and calix[4]arene biscrown **2** in the presence of a catalytic amount of TFA, followed by oxidation in situ with chloranil and further reaction with boron trifluoride etherate in the presence of ethyldiisopropylamine. The Calix-BODIPY-S was synthesized by condensation of the calix[4]arene biscrown **2** with 1,3-dimethylbodipy[28] under basic condition using piperidine in refluxing toluene in nonoptimized yield (12%).

Photophysical Properties of the Ligands. The photophysical studies of Calix-BODIPY and Calix-BODIPY-S were performed in CH_3CN and in a mixture of CH_3CN/CH_2Cl_2 9:1, respectively, in order to have a good solubility of the ligands. The absorption and fluorescence spectra of Calix-BODIPY and Calix-BODIPY-S ligands are shown in Figure 2 and their

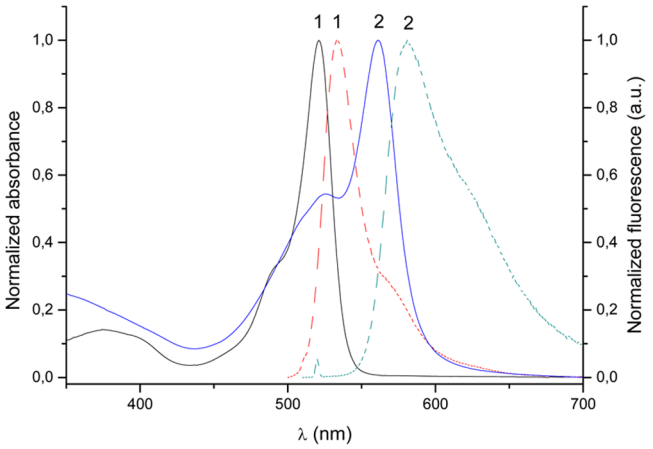

Figure 2. Absorption and emission spectra of Calix-BODIPY in CH_3CN (λ_{exc} = 527 nm) (1) and Calix-BODIPY-S in CH_3CN/CH_2Cl_2 9:1 (λ_{exc} = 550 nm) (2).

photophysical characteristics are summarized in Table 1. All the fluorophores show typical absorption features of BODIPY dyes, with an intense absorption band in the visible region corresponding to a $\pi \rightarrow \pi^*$ transition and a vibrational shoulder at a higher energy. The measured absorption coefficient of this transition is 64000 and 102000 L mol^{-1} cm^{-1} for Calix-BODIPY-S and Calix-BODIPY, respectively, which is in agreement with typical values of the BODIPY $\pi \rightarrow \pi^*$ transition.[21] They also possess the characteristic emission features of BODIPY: narrow and weakly Stokes-shifted band of mirror image shape and a high fluorescence quantum yield. The Calix-BODIPY has sharp absorption and emission bands with a maximum at 520 and 533 nm, respectively. A red shift of absorption and emission spectra with a maximum at 561 and 583 nm, respectively, is observed for Calix-BODIPY-S compound attributed to the extension of degree of π-conjugation. The absorption and emission maximums are almost the same as those of styryl-derivatized BODIPY compounds synthesized by Chang and co-workers.[28]

Solvatochromism effects of Calix-BODIPY-S were studied. A red shift accompanied by a broadening of emission band was observed with increasing solvent polarity (see the Supporting Information), indicating a small charge transfer character in this molecule. This effect is similar but less pronounced as compared to analogue dimethylamino styryl-substituted BODIPY due to a weaker electron-donating character of oxygen atom.[31] Time-resolved fluorescence measurements were performed by the single-photon counting method with picosecond laser excitation; the fluorescence decays for these calixarenes are shown in Figure 3. Satisfactory fits can be

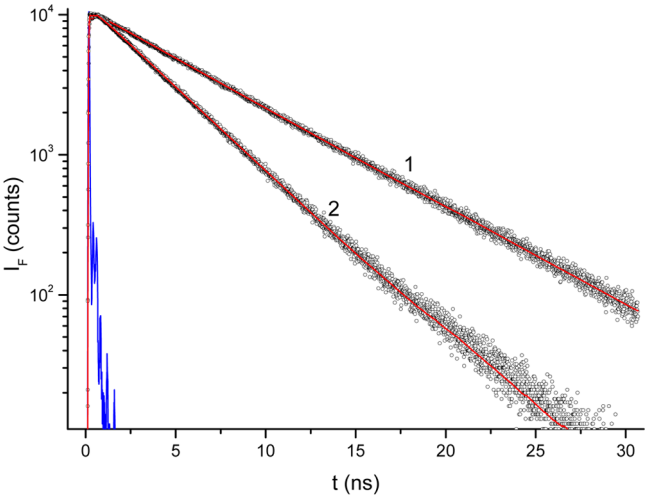

Figure 3. Fluorescence decays (λ_{exc} = 500 nm) of Calix-BODIPY (λ_{em} = 533 nm) and Calix-BODIPY-S (λ_{em} = 580 nm).

obtained by considering a single exponential (χ^2_R < 1.25), indicating the presence of only one emitting species. The radiative and nonradiative rate constants are related to the corresponding emission quantum yield and lifetime by $k_r = \Phi_F/\tau$ and $k_{nr} = (1-\Phi_F)/\tau$. The lower fluorescence quantum yield and lifetime of Calix-BODIPY-S compared to Calix-BODIPY is due to an increase in nonradiative rate constant that could probably be explained by its elongated π-conjugated system. Similarly, a decrease of quantum yield was also observed for BODIPY derivatives with an extension of the π-conjugated chain,[32−34] and this behavior was explained by an increase of intramolecular rotations which deactivate the excited state nonradiatively.[32]

Modeling. In order to demonstrate the conjugation effect between the coordination site and the signaling unit BODIPY in these two systems, we performed theoretical calculations within the DFT method (B3LYP) using the 6-31g(d) basis set by means of Gaussian 09. The calculations were performed on a simplified BODIPY fluorophore of these two calixarenes (BODIPY and BODIPY-S), in which the complexation site is replaced by two methoxy groups substituted on the benzene ring (Figure 4). For the BODIPY fluorophore, the *meso*-phenyl ring was found to be almost perpendicular (angle 85°) to the BODIPY plan. In contrast, the styryl function is nearly coplanar

Table 1. Photophysical Properties of Calix-BODIPY in CH_3CN and Calix-BODIPY-S in CH_3CN/CH_2Cl_2 9:1

product	λ_{abs}^{max} (nm)	λ_{fluo}^{max} (nm)	Φ_F	ε (L mol^{-1} cm^{-1})	τ (ns)	k_r (10^8 s^{-1})	k_{nr} (10^8 s^{-1})
Calix-BODIPY	520	533	0.81	102000	6.07	1.33	0.31
Calix-BODIPY-S	561	581	0.48	64000	3.62	1.33	1.44

DOI: 10.1021/jp5120288
J. Phys. Chem. A XXXX, XXX, XXX−XXX

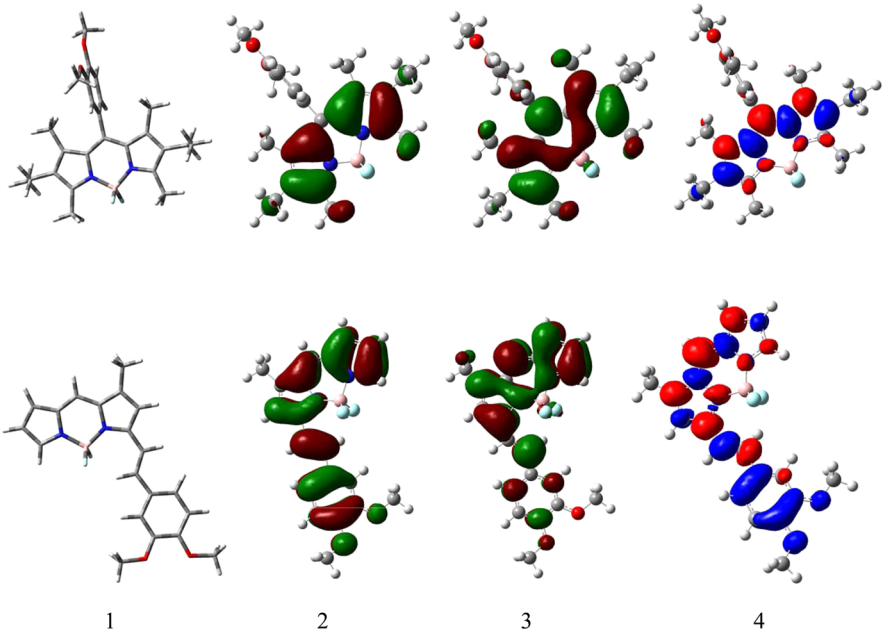

Figure 4. (1) Optimized ground state geometries, (2) HOMO, (3) LUMO, and (4) electron density changes associated with the first electronic transition of model BODIPY (top) and model BODIPY-S (bottom).

with the BODIPY, with a twist of 13°. The optimized ground state geometries, HOMO and LUMO orbitals, are illustrated in Figure 4.

In the case of the model BODIPY-S, the electronic density is delocalized both on the BODIPY and the styryl moiety for the HOMO. The LUMO is localized essentially in the BODIPY moiety, and the electronic density in styryl moiety is smaller than in the HOMO, indicating a charge transfer character from the styryl moiety to the BODIPY core in this molecule. Conversely, both HOMO and LUMO are mainly localized only in the BODIPY moiety for the model BODIPY (top in Figure 4) since the conjugation is interrupted with the *meso*-phenyl, which is orthogonal to the BODIPY plane, canceling the delocalization of electronic distribution on the oxygen atoms.

In order to justify the contribution of the oxygen atoms in the charge delocalization process in the excited state for these two compounds, TD-DFT method using the PBE0 functional with a 6-311+g(d,p) basis set was performed to examine electronic transitions.[24] We present in Figure 4 the difference of total electronic density between the first excited state and the ground state of these two molecules. In the case of BODIPY-S, the electronic density decreases (blue) at the styryl moiety, while it mainly localizes on the BODIPY core (red) in the excited stated. Conversely, there is no important contribution of the electronic density in the oxygen atoms substituted at the *meso*-phenyl ring of the BODIPY fluorophore, in agreement with the small spectral change in the presence of cations.

Complexing Properties. The complexation studies of potassium and cesium with Calix-BODIPY and Calix-BODIPY-S were performed in CH_3CN and in a mixture of CH_3CN/CH_2Cl_2 9:1, respectively. The evolution of absorption and emission spectra of Calix-BODIPY and Calix-BODIPY-S upon complexation with Cs^+ are displayed in Figures 5 and 6, respectively. The insets in Figures 5b and 6b show the increase of fluorescence intensity upon progressive addition of Cs^+ ions.

Addition of K^+ and Cs^+ induces a slight bathochromic shift in absorption and fluorescence spectra of Calix-BODIPY as shown in Figure 5. Binding of these cations to this ligand accompanies only a small increase in fluorescence quantum yield and practically no change in fluorescence decay time. On the other hand, cation complexation in the case of Calix-BODIPY-S induces a more pronounced hypsochromic shift of absorption and fluorescence spectra. In line with this spectral shift, a strong increase of the fluorescence quantum yield was also observed in the presence of cations. The different behavior of these two BODIPY-based ligands can be explained as follows. Let us look at the structural difference between the two molecules. The substantial difference between the structures of these two ligands is the position of coordination site introduced to the BODIPY core. In Calix-BODIPY, the ionophore is introduced at the *meso* position, while it is substituted at the α position in Calix-BODIPY-S ligand. Theoretical calculations described above and X-ray structure experiments show that the phenyl ring at the *meso* position is twisted out of the plane with respect to BODIPY chromophore when the methyl groups are present at the β position.[35,36] As a consequence, the conjugation between oxygen atoms of the crown-ether coordination site and the BODIPY chromophore is interrupted in Calix-BODIPY.

Thus, this interruption of conjugation can explain the very slight changes in the photophysical properties of this ligand in the presence of the cation. The only effect that can be produced upon cation complexation is the inductive effect on the crown-ether coordination site. Indeed, theoretical calculations showed that the highest occupied molecular orbital (HOMO) is always localized on the BODIPY core, and its energy is slightly influenced by the effect of the substitution of the *meso*-phenyl group. However, the lowest unoccupied molecular orbital (LUMO) is more localized on the phenyl group, and its energy is lower with acceptor substituents on *meso*-phenyl ring.[36] Therefore, the HOMO−LUMO transition energy is lower when one increases the acceptor capacity of phenyl substituents. In our case, binding of cations to the crown-ether reduces the electron-donating character of oxygen atoms and, therefore, results in the slight bathochromic shift observed on absorption and fluorescence spectra of Calix-BODIPY. However, the spectral change is small as the crown-ether

DOI: 10.1021/jp5120288
J. Phys. Chem. A XXXX, XXX, XXX−XXX

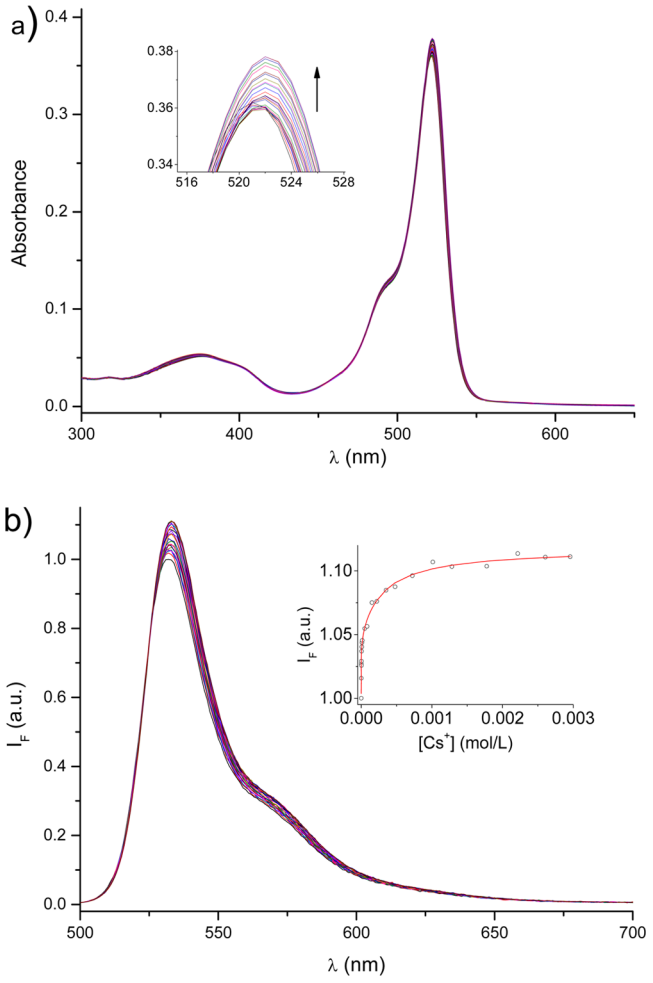

Figure 5. Evolution of (a) absorption (3.6×10^{-6} M) and (b) emission spectrum (1.1×10^{-6} M) of Calix-BODIPY upon addition of cesium perchlorate in CH_3CN, λ_{exc} = 527 nm. Inset: (a) zoom of absorption spectra around 520 nm and (b) calibration curve as a function of cesium concentration, λ_{em} = 533 nm.

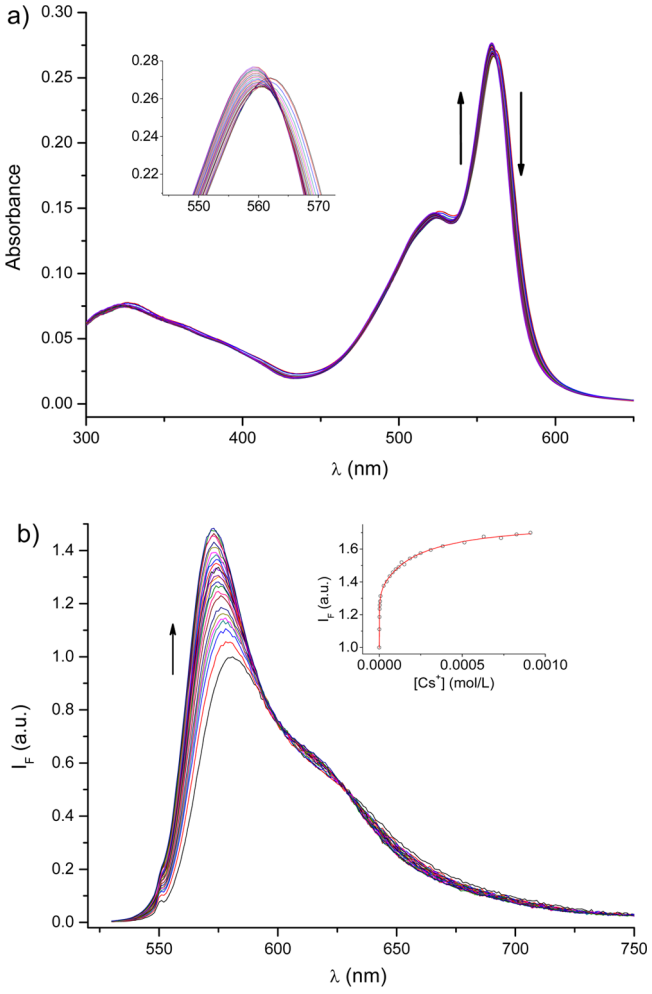

Figure 6. Evolution of (a) absorption (3.9×10^{-6} M) and (b) emission spectrum (1.3×10^{-6} M) of Calix-BODIPY-S upon addition of cesium perchlorate in CH_3CN/CH_2Cl_2 9:1, λ_{exc} = 550 nm. Inset: (a) zoom of absorption spectra around 560 nm, (b) calibration curve as a function of cesium concentration at λ_{em} = 573 nm.

coordination site is not directly conjugated to the BODIPY signaling unit.

In contrast, calculations showed that the crown-ether (electron-donating group) and the BODIPY signaling unit (electron-withdrawing group) in Calix-BODIPY-S are electronically conjugated, and this molecule presents a charge delocalization effect between the oxygen atoms of the coordination site and the BODIPY fluorophore. Therefore, important shifts in absorption and fluorescence spectra were observed in the presence of cations. Binding with Cs^+ induces a 3 and 8 nm hypsochromic shifts of the absorption and emission spectra, respectively. Similar effects are also observed for the complexation with K^+. The interaction of cation with oxygen atoms decreases their electron-donating character and reduces the efficiency of the charge delocalization, resulting in a hypsochromic shift of the spectra.

Careful analysis of the emission spectra upon addition of the cations by means of SPECFIT software reveals that different complexes are formed with 1:1 and 2:1 stoichiometries, which are in agreement with the two crown-ether complexation sites. Table 2 presents stability constants of the complexes formed with the K^+ and Cs^+ cations, calculated from the results of the titration experiments. It is interesting to notice that the stability constants of the complexes with Calix-BODIPY and Calix-BODIPY-S are similar and in agreement with those previously observed for similar calix[4]arene biscrown-6 ether with the same coordination site.[14,37] The greater stability constants observed for the Cs^+ cations than those for K^+ cations can be explained in terms of the cation radius as previously reported. In fact, the Cs^+ cations fit perfectly in the cavity of crown ether, while the size of K^+ is smaller and thus the complexes with Cs^+ are more stable. These stability constants are higher compared to those of BODIPY-substituted crown-ether sensors previously studied in the literature[38,39] since these calixcrowns combining calixarene and crown ether frameworks are more rigid and present a better selectivity for alkali cations.

The fluorescence spectra of the 1:1 and 2:1 complexes of Calix-BODIPY and Calix-BODIPY-S with Cs^+ are provided by data analysis using SPECFIT. These spectra are shown in Figure 7 together with the spectrum of the free ligands. The fluorescence spectrum of the 1:1 complex is almost half sum with respect to the spectrum of the free ligand and that of 2:1 complex for both two calixarenes, indicating that the two binding sites have the same affinities for cations. The SPECFIT software also provides the molar fractions of species including free ligand (L), 1:1 complex (ML), and 2:1 complex (M_2L) for

DOI: 10.1021/jp5120288
J. Phys. Chem. A XXXX, XXX, XXX−XXX

Table 2. Stability Constants of the Complexes of Calix-BODIPY and Calix-BODIPY-S with Cesium and Potassium Perchlorate

ligand	cation	ionic radius (Å)	log K_{11}	log K_{21}	log β_{21}
Calix-BODIPY	Cs^+	1.67	5.87 ± 0.05	3.5 ± 0.2	9.41 ± 0.07
	K^+	1.38	4.30 ± 0.05	2.3 ± 0.3	6.6 ± 0.2
Calix-BODIPY-S	Cs^+	1.67	6.09 ± 0.04	3.7 ± 0.2	9.78 ± 0.07
	K^+	1.38	4.67 ± 0.03	2.4 ± 0.1	7.10 ± 0.07

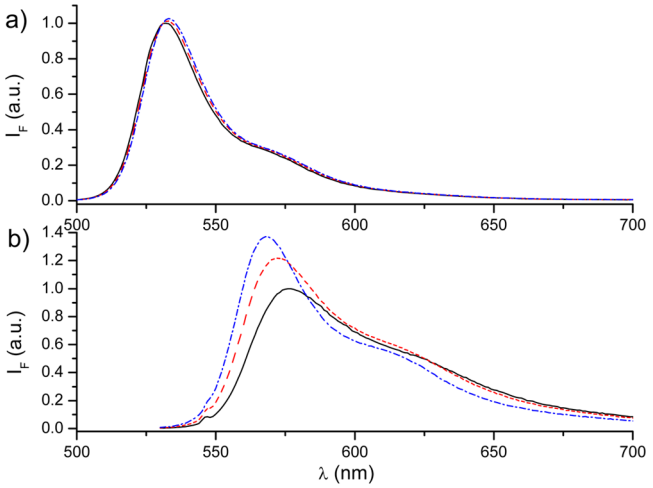

Figure 7. Emission spectra of the 1:1 and 2:1 complexes of (a) Calix-BODIPY and (b) Calix-BODIPY-S calculated from the titration data analysis using the SPECFIT software.

different concentrations of Cs^+. The evolution of these fractions with increasing concentrations of Cs^+ is presented in Figure 8.

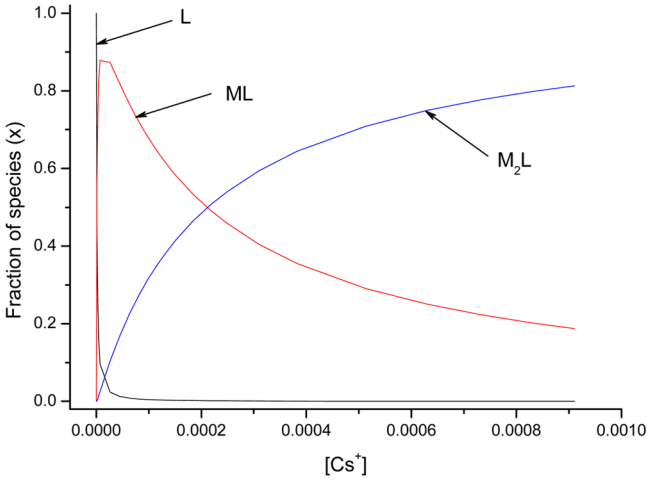

Figure 8. Distribution curves of Calix-BODIPY-S (1.3×10^{-6} M) and its 1:1 and 2:1 complexes with Cs^+.

At a high concentration of cations, the most predominant species in solution is the M_2L complex, and the free ligand L completely disappears. The distribution curves of the species will be used later to understand the results obtained by time-resolved fluorescence measurements.

The fluorescence decays of Calix-BODIPY and Calix-BODIPY-S with increasing Cs^+ or K^+ concentration were studied in the same condition as steady-state measurements. The fluorescence quantum yield and the lifetime of the 2:1 complexes with the cations are given in Table 3. The fluorescence decay time of Calix-BODIPY in the presence of

Table 3. Photophysical Parameters of Calix-BODIPY and Calix-BODIPY S and Their Complexes with K^+ and Cs^+

ligand	cation	Φ_F	τ (ns)	k_r (10^8 s^{-1})	k_{nr} (10^8 s^{-1})
Calix-BODIPY		0.81	6.07	1.33	0.31
	Cs^+	0.83	6.08	1.37	0.28
	K^+	0.82	6.01	1.36	0.30
Calix-BODIPY-S		0.48	3.62	1.33	1.44
	Cs^+	0.52	3.85	1.35	1.25
	K^+	0.52	3.82	1.36	1.26

cations is almost unchanged, which is in agreement with the slight spectral changes previously observed. Instead, the fluorescence lifetime of the 2:1 complex excited state was increased to 3.85 and 3.82 ns for Cs^+ and K^+, respectively, compared to the free Calix-BODIPY-S of the 3.62 ns lifetime. This increase is in line with the exaltation in fluorescence intensity and can be related to a decrease of nonradiative constants in the complexes.

Assuming the two complexation sites are equivalent, we can consider that the 1:1 complex contains two different sites. The one without cation has the same decay time as the free ligand, and the other in interaction with a bound cation has the same lifetime as the 2:1 complex. A biexponential decay is expected.

$$I(t) = \alpha_1 \exp(-t/\tau_1) + \alpha_2 \exp(-t/\tau_2) \text{ with } \Sigma\alpha_i = 1$$

where τ_1 is the lifetime of a BODIPY moiety in the free ligand and τ_2 is the lifetime of a BODIPY moiety in interaction with Cs^+ in the ML and M_2L complexes. The fluorescence decays with increasing Cs^+ concentration were then fitted with biexponential functions with a shorter lifetime τ_1 = 3.62 ns corresponding to the free BODIPY moiety and a longer decay time τ_2 = 3.85 ns corresponding to the BODIPY moiety in interaction with Cs^+. Figure 9 shows the evolution in function of Cs^+ concentration of the preexponential coefficients, α_1 and α_2, for these two decay times τ_1 and τ_2. Thanks to the stability constants determined by steady-state fluorescence measurements, the evolution of preexponential coefficients α_1 and α_2 can be related to the relative proportions of the free ligand and its complexes, ML and ML_2, by using the following relations:

$$\alpha_1 = x_L + x_{ML}/2$$

$$\alpha_2 = x_{M2L} + x_{ML}/2$$

where x_L, x_{ML}, and x_{M2L} are the proportions of the different species related to the given concentration of Cs^+ and the stability constants as demonstrated in Figure 8. The lifetime of the free ligand form was found to completely disappear in high Cs^+ concentration as we can see from the evolution of preexponential coefficients in Figure 9. These evolutions are perfectly compatible with the value of the stability constants determined by steady-state measurements.

This result shows that the two complexation sites are completely equivalent, and there is no difference in photophysical properties between the 1:1 and 2:1 complexes. It also indicates that there is no presence of the photoejection of

DOI: 10.1021/jp5120288
J. Phys. Chem. A XXXX, XXX, XXX−XXX

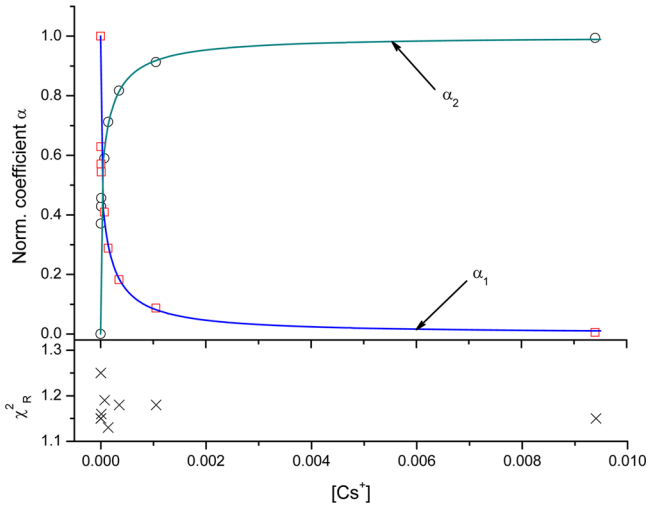

Figure 9. Global analysis of fluorescence decay of Calix-BODIPY-S upon addition of Cs^+ in CH_3CN/CH_2Cl_2 9:1, λ_{exc} = 500 nm, λ_{em} = 580 nm. The analysis was performed with some of two discrete exponentials. The ° and □ symbols represent the evolution of the preexponential coefficients as a function of Cs^+ concentration. The solid lines represent the proportion of the free ligand and the ligand bound to Cs^+ cation, obtained from the stability constants.

bound cation in the excited-state complexes as previously observed for fluoroionophores where a bound cation is in interaction with an electron-donating group conjugated with an electron-withdrawing group.[40,41] Indeed, the oxygen atoms of the crown-ether play double roles: they participate as an electron-donating group in the photoinduced charge transfer process to the BODIPY moiety and they also serve as binding sites to cations. In the excited state, the photoinduced charge transfer process reduces the electron density on the electron-donating group, resulting in a reduction of coordination strength and the cation maybe even ejected from the binding site. In this case, we would observe the following results: (i) the fluorescence spectrum of the 1:1 complex would be different from the average of the spectra corresponding to free ligand and 2:1 complex; (ii) the fluorescence spectra of the complex is only slightly blue-shifted; and (iii) the fluorescence decay would be a sum of at least three exponentials: the free ligand, the ligand in interaction with the cation, and the ligand that undergoes cation photoejection. However, none of these results were observed for the complexation properties of Calix-BODIPY-S. Therefore, our photophysical studies by steady-state and time-resolved fluorescence show that there is likely no possibility of cation ejection in the excited state of the complexes. The weaker electron-donating character of the oxygen atom as compared to the nitrogen atom and the longer distance between donor and acceptor moieties in Calix-BODIPY-S compared to previously observed structures[40,41] are the possible reasons for the absence of cation photoejection in our case.

CONCLUSION

In summary, we have successfully synthesized two new sensors for alkali cations based on the BODIPY fluorophore. Photophysical investigation of free ligands and their complexes with cesium and potassium were performed by steady-state and time-resolved fluorescence studies. These molecules have interesting photophysical properties with a relatively high absorption coefficient and a good fluorescence quantum yield. It was observed that the coordination site introduced at α-position of the BODIPY core has a better response to the complexation with cations, as the calix[4]biscrown-6 ether is electronically conjugated to the BODIPY fluorophore (Calix-BODIPY-S). The hypsochromic shift of absorption and fluorescence spectra of Calix-BODIPY-S is attributed to the binding of cation to the crown-ether groups, which reduces the electron-donating character of oxygen atoms conjugated to the BODIPY fluorophore. These ligands present a high stability constant with cesium cations (log K_{11} = 6.09 for calix-BODIPY-S) and a good selectivity toward the cesium ion versus the potassium ion. The photodisruption of the interaction between the bound cation and the oxygen atoms of the coordination site is not observed. Works are in progress to introduce water-soluble groups in these sensors in order to detect alkali cations in aqueous media.

ASSOCIATED CONTENT

Supporting Information

Solvatochromism study and Cartesian coordinates of the optimized structures. This material is available free of charge via the Internet at http://pubs.acs.org.

AUTHOR INFORMATION

Corresponding Authors

*E-mail: minh-huong.ha-thi@u-psud.fr.
*E-mail: isabelle.leray@ppsm.ens-cachan.fr.

Notes

The authors declare no competing financial interest.

ACKNOWLEDGMENTS

This work was supported by the National Research Agency program "DECRET". The authors are grateful to A. Brosseau for his assistance in tuning the single-photon timing instrument. We thank R. Meallet-Renault, G. Clavier, and J. P. Lefevre for fruitful discussions.

REFERENCES

(1) Miyazaki, H.; Kato, H.; Kato, Y.; Tsuchiyama, T.; Terada, H. Estimation of the Intake of Radioactive Cesium Based on Analysis of Total Diet Samples in Nagoya. *J. Food. Soc. Jpn.* **2013**, *54*, 151−155.
(2) Melnikov, P.; Zanoni, L. Z. Clinical Effects of Cesium Intake. *Biol. Trace Elem. Res.* **2010**, *135*, 1−9.
(3) Groll, H.; Schnurerpatschan, C.; Kuritsyn, Y.; Niemax, K. Wavelength Modulation Diode-Laser Atomic-Absorption Spectrometry in Analytical Flames. *Spectrochim. Acta, Part B* **1994**, *49*, 1463−1472.
(4) Van Renterghem, D.; Cornelis, R.; Vanholder, R. Radiochemical Determination of Twelve Trace Elements in Human Blood Serum. *Anal. Chim. Acta* **1992**, *257*, 1−5.
(5) Theimer, K. H.; Krivan, V. Determination of Uranium, Thorium, and 18 Other Elements in High-Purity Molybdenum by Radiochemical Neutron Activation Analysis. *Anal. Chem.* **1990**, *62*, 2722−2727.
(6) de Silva, A. P.; Gunaratne, H. Q. N.; Gunnlaugsson, T.; Huxley, A. J. M.; McCoy, C. P.; Rademacher, J. T.; Rice, T. E. Signaling Recognition Events with Fluorescent Sensors and Switches. *Chem. Rev.* **1997**, *97*, 1515−1566.
(7) Valeur, B.; Leray, I. Design Principles of Fluorescent Molecular Sensors for Cation Recognition. *Coord. Chem. Rev.* **2000**, *205*, 3−40.
(8) Kim, H. N.; Ren, W. X.; Kim, J. S.; Yoon, J. Fluorescent and Colorimetric Sensors for Detection of Lead, Cadmium, and Mercury Ions. *Chem. Soc. Rev.* **2012**, *41*, 3210−3244.

DOI: 10.1021/jp5120288
J. Phys. Chem. A XXXX, XXX, XXX−XXX

(9) Leray, I.; Valeur, B. Calixarene-Based Fluorescent Molecular Sensors for Toxic Metals. *Eur. J. Inorg. Chem.* **2009**, 3525−3535.
(10) Ungaro, R.; Casnati, A.; Ugozzoli, F.; Pochini, A.; Dozol, J.-F.; Hill, C.; Rouquette, H. 1,3-Dialkoxycalix[4]Arenecrowns-6 in 1,3-Alternate Conformation: Cesium-Selective Ligands That Exploit Cation-Arene Interactions. *Angew. Chem., Int. Ed. Engl.* **1994**, *33*, 1506−1509.
(11) Asfari, Z.; Thuéry, P.; Nierlich, M.; Vicens, J. Unsymmetrical Calix[4]-Bis-Crowns-6 with Unequivalent Crown Loops. *Tetrahedron Lett.* **1999**, *40*, 499−502.
(12) Talanov, V. S.; Talanova, G. G.; Gorbunova, M. G.; Bartsch, R. A. Novel Caesium-Selective, 1,3-Alternate Calix[4]Arene-Bis(Crown-6-Ethers) with Proton-Ionizable Groups for Enhanced Extraction Efficiency. *J. Chem. Soc., Perkin Trans. 2* **2002**, 209−215.
(13) Souchon, V.; Leray, I.; Valeur, B. Selective Detection of Cesium by a Water-Soluble Fluorescent Molecular Sensor Based on a Calix 4 Arene-Bis(Crown-6-Ether). *Chem. Commun.* **2006**, 4224−4226.
(14) Leray, I.; Asfari, Z.; Vicens, J.; Valeur, B. Synthesis and Binding Properties of Calix 4 Biscrown-Based Fluorescent Molecular Sensors for Caesium or Potassium Ions. *J. Chem. Soc., Perkin Trans. 2* **2002**, 1429−1434.
(15) Wu, T.; Zhao, L. Y.; Faye, D.; Lefevre, J. P.; Delaire, J.; Leray, I. Determination of Lead in Water by Combining Precolumn Adsorption and Fluorimetric Detection in a Microfluidic Device. *Anal. Methods* **2012**, *4*, 989−994.
(16) Faye, D.; Lefevre, J. P.; Delaire, J. A.; Leray, I. A Selective Lead Sensor Based on a Fluorescent Molecular Probe Grafted on a Pdms Microfluidic Chip. *J. Photochem. Photobiol., A* **2012**, *234*, 115−122.
(17) Boens, N.; Leen, V.; Dehaen, W. Fluorescent Indicators Based on Bodipy. *Chem. Soc. Rev.* **2012**, *41*, 1130−1172.
(18) Sculimbrene, B. R.; Imperiali, B. Lanthanide-Binding Tags as Luminescent Probes for Studying Protein Interactions. *J. Am. Chem. Soc.* **2006**, *128*, 7346−7352.
(19) Zhou, Y.; Xiao, Y.; Li, D.; Fu, M.; Qian, X. Novel Fluorescent Fluorine−Boron Complexes: Synthesis, Crystal Structure, Photoluminescence, and Electrochemistry Properties. *J. Org. Chem.* **2008**, *73*, 1571−1574.
(20) Yang, Y.; Zhang, L.; Li, B.; Zhang, L.; Liu, X. Triphenylamine-Cored Tetramethyl-Bodipy Dyes: Synthesis, Photophysics and Lasing Properties in Organic Media. *RSC Adv.* **2013**, *3*, 14993−14996.
(21) Ulrich, G.; Ziessel, R.; Harriman, A. The Chemistry of Fluorescent Bodipy Dyes: Versatility Unsurpassed. *Angew. Chem., Int. Ed.* **2008**, *47*, 1184−1201.
(22) Loudet, A.; Burgess, K. Bodipy Dyes and Their Derivatives: Syntheses and Spectroscopic Properties. *Chem. Rev.* **2007**, *107*, 4891−4932.
(23) Frisch, M.; Trucks, G.; Schlegel, H.; Scuseria, G.; Robb, M.; Cheeseman, J.; Scalmani, G.; Barone, V.; Mennucci, B.; Petersson, G., et al., *Gaussian 09*, revision D. 01; Gaussian: Wallingford, CT, 2013.
(24) Jacquemin, D.; Perpète, E. A.; Ciofini, I.; Adamo, C. Accurate Simulation of Optical Properties in Dyes. *Acc. Chem. Res.* **2008**, *42*, 326−334.
(25) Kubin, R. F.; Fletcher, A. N. Fluorescence Quantum Yields of Some Rhodamine Dyes. *J. Lumin.* **1982**, *27*, 455−462.
(26) Gampp, H.; Maeder, M.; Meyer, C. J.; Zuberbühler, A. D. Calculation of Equilibrium Constants from Multiwavelength Spectroscopic Data—I: Mathematical Considerations. *Talanta* **1985**, *32*, 95−101.
(27) Bu, J.-H.; Zheng, Q.-Y.; Chen, C.-F.; Huang, Z.-T. The Synthesis of Calix[4]Crown Based Dendrimer. *Tetrahedron* **2005**, *61*, 897−902.
(28) Lee, J.-S.; Kang, N.-y.; Kim, Y. K.; Samanta, A.; Feng, S.; Kim, H. K.; Vendrell, M.; Park, J. H.; Chang, Y.-T. Synthesis of a Bodipy Library and Its Application to the Development of Live Cell Glucagon Imaging Probe. *J. Am. Chem. Soc.* **2009**, *131*, 10077−10082.
(29) Kollmannsberger, M.; Rurack, K.; Resch-Genger, U.; Daub, J. Ultrafast Charge Transfer in Amino-Substituted Boron Dipyrromethene Dyes and Its Inhibition by Cation Complexation: A New Design Concept for Highly Sensitive Fluorescent Probes. *J. Phys. Chem. A* **1998**, *102*, 10211−10220.
(30) Dumas-Verdes, C.; Miomandre, F.; Lépicier, E.; Galangau, O.; Vu, T. T.; Clavier, G.; Méallet-Renault, R.; Audebert, P. Bodipy-Tetrazine Multichromophoric Derivatives. *Eur. J. Inorg. Chem.* **2010**, *2010*, 2525−2535.
(31) Rurack, K.; Kollmannsberger, M.; Daub, J. Molecular Switching in the near Infrared (Nir) with a Functionalized Boron−Dipyrromethene Dye. *Angew. Chem., Int. Ed.* **2001**, *40*, 385−387.
(32) Hu, R.; Lager, E.; Aguilar-Aguilar, A. l.; Liu, J.; Lam, J. W. Y.; Sung, H. H. Y.; Williams, I. D.; Zhong, Y.; Wong, K. S.; Peña-Cabrera, E.; et al. Twisted Intramolecular Charge Transfer and Aggregation-Induced Emission of Bodipy Derivatives. *J. Phys. Chem. C* **2009**, *113*, 15845−15853.
(33) Zhu, S.; Zhang, J.; Vegesna, G.; Luo, F.-T.; Green, S. A.; Liu, H. Highly Water-Soluble Neutral Bodipy Dyes with Controllable Fluorescence Quantum Yields. *Org. Lett.* **2010**, *13*, 438−441.
(34) Buyukcakir, O.; Bozdemir, O. A.; Kolemen, S.; Erbas, S.; Akkaya, E. U. Tetrastyryl-Bodipy Dyes: Convenient Synthesis and Characterization of Elusive Near IR Fluorophores. *Org. Lett.* **2009**, *11*, 4644−4647.
(35) Kollmannsberger, M.; Gareis, T.; Heinl, S.; Daub, J.; Breu, J. Electrogenerated Chemiluminescence and Proton-Dependent Switching of Fluorescence: Functionalized Difluoroboradiaza-S-Indacenes. *Angew. Chem., Int. Ed. Engl.* **1997**, *36*, 1333−1335.
(36) Galangau, O.; Dumas-Verdes, C.; Meallet-Renault, R.; Clavier, G. Rational Design of Visible and NIR Distyryl-Bodipy Dyes from a Novel Fluorinated Platform. *Org. Biomol. Chem.* **2010**, *8*, 4546−4553.
(37) Pellet-Rostaing, S.; Chitry, F.; Nicod, L.; Lemaire, M. Synthesis and Complexation Properties of 1,3-Alternate Calix 4 Arene-Bis(Crown-6) Derivatives. *J. Chem. Soc., Perkin Trans. 2* **2001**, 1426−1432.
(38) Yamada, K.; Nomura, Y.; Citterio, D.; Iwasawa, N.; Suzuki, K. Highly Sodium-Selective Fluoroionophore Based on Conformational Restriction of Oligoethyleneglycol-Bridged Biaryl Boron-Dipyrromethene. *J. Am. Chem. Soc.* **2005**, *127*, 6956−6957.
(39) Kollmannsberger, M.; Rurack, K.; Resch-Genger, U.; Rettig, W.; Daub, J. Design of an Efficient Charge-Transfer Processing Molecular System Containing a Weak Electron Donor: Spectroscopic and Redox Properties and Cation-Induced Fluorescence Enhancement. *Chem. Phys. Lett.* **2000**, *329*, 363−369.
(40) Valeur, B.; Leray, I.; Zhao, L. Y.; Souchon, V.; Metivier, R.; Plaza, P.; Ley, C.; Lacombat, F.; Martin, M. M. Photoinduced Cation Translocation in a Calix[4]Biscrown: Towards a New Type of Light-Driven Molecular Shuttle. *ChemPhysChem* **2010**, *11*, 2416−2423.
(41) Leray, I.; Asfari, Z.; Vicens, J.; Valeur, B. Photophysics of Calix 4 Biscrown-Based Ditopic Receptors of Caesium Containing One or Two Dioxocoumarin Fluorophores. *J. Fluoresc.* **2004**, *14*, 451−458.

DOI: 10.1021/jp5120288
J. Phys. Chem. A XXXX, XXX, XXX−XXX